Chapter 7

Effect of MWCNT on Thermo-Mechanical, Electrical and EMI-SE of BMI-EpoxyComposites with Different Nanofillers

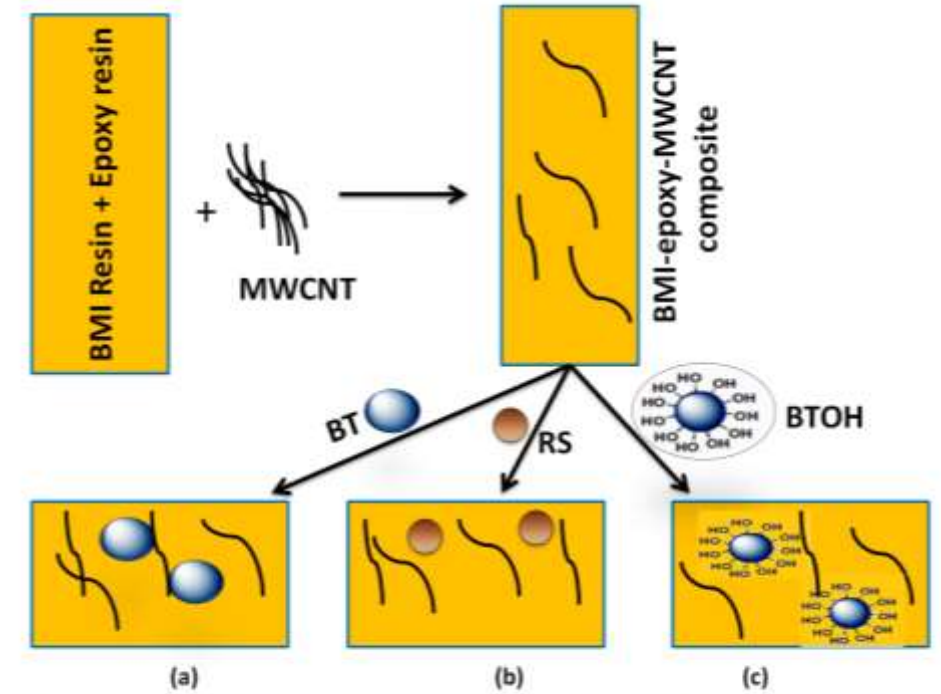

BMI-epoxy-MWCNT composite with (a) BT (b) RS (c) BTOH filler

Chapter 7

Effect of MWCNT on Thermo–Mechanical, Electrical and EMI-SE of BMI-Epoxy Nanocomposites with Different Nanofillers

Abstract

Attempts were made to improve the thermo-mechanical, dielectric and electromagnetic interference shielding effectiveness (EMI-SE) of bismaleimide (BMI)-epoxy composites using different fillers such as $BaTiO_3$ (BT), Rochelle salt (RS) and surface hydroxylated $BaTiO_3$ (BTOH) along with the incorporation of conductive filler multiwalled carbon nanotube (MWCNT) as secondary reinforcement and silane coated E glass fiber (SC-EGF) as the primary reinforcement. Based on our previous work in chapter 4, 5 and 6 fabrication of BMI-epoxy composites with different nanofiller (1 - 5 weight %) were done and we got highest tensile strength, flexural strength and dielectric constant at 2 weight % of filler loading and highest dielectric strength at 3 weight % of nanofiller. BMI-epoxy nanocomposites containing 5 weight % of MWCNT with optimized 2 and 3 weight % of BT, RS and BTOH fillers were fabricated using hand layup method followed by compression moulding. The resulting composites were characterized to explore the influence of MWCNT on thermal, mechanical, dielectric properties and EMI-SE. Tensile strength, flexural strength and dielectric permittivity of BMI-epoxy-MWCNT nanocomposite with 2 weight % of BTOH nanofiller have increased 2.78, 1.22 and 1.50 times respectively as compared to BMI-epoxy-BTOH nanocomposite without MWCNT filler. The highest dielectric permittivity of around 674 and minimum value of dielectric loss of 0.017 were obtained for BMI-epoxy-MWCNT composite with BTOH nanofiller and this composite stands as a promising candidate for high dielectric applications.

7.1. Introduction

Conductive polymer nanocomposites stand as attractive and advanced materials to protect electronic devices such as laptops, sensors, cell phones, military and aircraft devices etc. from electromagnetic interference and electrostatic discharge. Among the different conductive nanofillers such as carbon nanotubes (CNT)[1–6], metal nanowires[7,8],

carbon nanofibers (CNF)[9–11], high structure carbon black (HS-CB)[12], conventional carbon fibers (CF)[13,14] etc., the highest EMI-SE, dielectric permittivity and conductivity is exhibited by MWCNT nanocomposites because of its high aspect ratio and high intrinsic conductivity[15–17].

EMI-SE and conductivity of polyvinylchloride (PVC)-$BaTiO_3$-NiO nanocomposites by varying the compositions of the fillers $BaTiO_3$ and NiO were investigated by Aqib Muzaffar et al.[18] Maximum EMI-SE of 18.71 dB was obtained at 30 weight % of $BaTiO_3$ and 5 weight % of NiO. The enhancement in EMI-SE of the synthesized composites is due to the enhancement in conductivity in PVC-$BaTiO_3$-NiO that is attributed to the formation of conductive surface between polymer matrix by NiO filler and large surface area and dipoles provided by $BaTiO_3$ nanoparticles.

Qunfeng Cheng et al. investigated and compared the mechanical properties and electrical conductivity of epoxy functionalized MWCNT composites with different stretch alignment reinforced BMI composites with pristine CNT sheet/BMI composites. BMI-CNT composites with epoxy functionalized CNT sheets at 40% stretch showed highest tensile strength, Young's modulus and electrical conductivity as compared to pristine CNT sheet/BMI composites[19]. From these results, it is evident that degree of CNT alignment, CNT loading, CNT length and interfacial bonding will be critical in the fabrication of BMI-CNT composites for improving their mechanical properties as well as electrical conductivity[20–22].

Diallyl bisphenol A modified bismaleimide (BMI-BA)-CNT hybrid and BMI-BA with aminated CNT (A-CNT) were fabricated by Aijuan Gu et al. and studied the static and dynamic mechanical properties in detail. The obtained experimental data shows that the mechanical properties of the above composites were greatly influenced by the nature of functional groups on CNT and its loading in the matrix[22].

In our previous work, the effect of three different fillers such as $BaTiO_3$ (BT), Rochelle salt (RS) and surface hydroxylated $BaTiO_3$ (BTOH) nanoparticles on the thermo-mechanical, dielectric and EMI-SE of BMI-epoxy composites were studied. All the fillers enhance the above mentioned properties except EMI-SE. In this regard, a conductive filler, MWCNT is incorporated during the fabrication of the composite.

In this chapter, BMI-epoxy-MWCNT composites with different fillers with optimized weight % obtained from our previous work have been incorporated for the improved ac conductivity and EMI-SE of the composites.

7.2. Results and discussion

7.2.1. Thermogravimetric analysis of BMI-epoxy-MWCNT composites

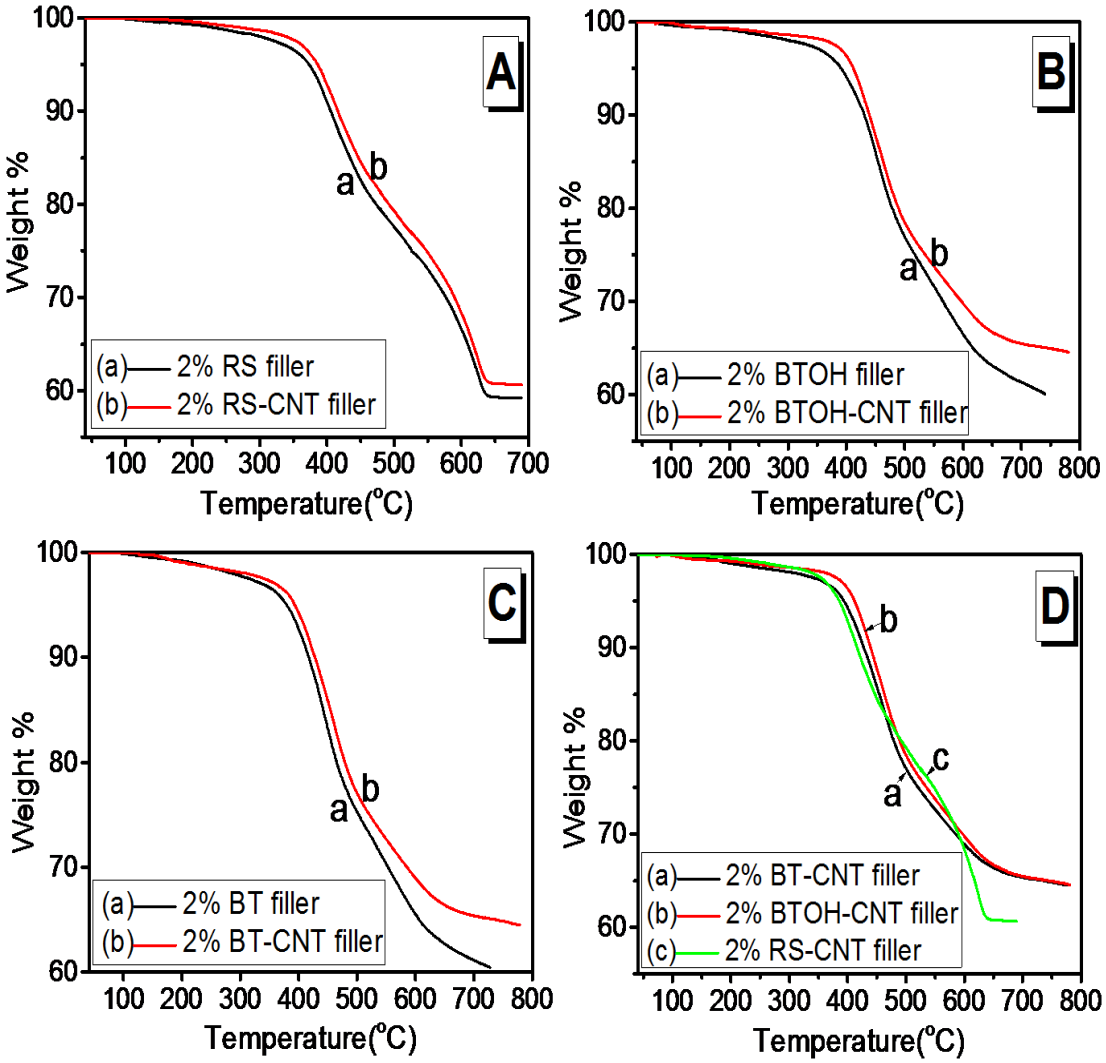

Figure 7.1 TGA curves of BMI-epoxy with and without MWCNT composites (A) RS filler, (B) BTOH nanofiller, (C) BT nanofiller, (D) Comparison of BMI-epoxy-MWCNT composites with (a) BT (b) BTOH and (c) RS filler.

The thermal stability of BMI-epoxy-MWCNT composites with different nanofillers such as BT, RS and BTOH were examined by analyzing the thermogravimetric curves of fabricated composites and are depicted in figure 7.1D. The thermal stability of

fabricated BMI-epoxy composites was synergistically enhanced by the addition of MWCNT filler which is evident from figures 7.1 A, B and C and from table 7.1[23,24].

Table 7.1 Tentative assignments from TGA curves of BMI-epoxy composites with different fillers such as BT, BTOH, RS with and without MWCNT fillers.

Sample	Decomposition temperature	Weight % of final residue at 688°C	Sample	Decomposition temperature	Weight % of final residue at 688°C
BMI-epoxy-BT composite	380 °C	61.42	BMI-epoxy-MWCNT-BT composite	395°C	65.48
BMI – epoxy BTOH composite	392°C	61.73	BMI-epoxy-MWCNT-BTOH composite	413°C	65.64
BMI – epoxy RS composite	374°C	59.2	BMI-epoxy-MWCNT-RS composite	386°C	60.60

7.2.2. FTIR spectra

FTIR spectra of BMI-epoxy-MWCNT composites with different fillers such as BT, RS and BTOH are illustrated in figure 7.2. Compared with FTIR spectrum of BMI-epoxy composites, the absorption bands correspond to -CH=CH- stretching of maleimide ring at 823 cm^{-1}, weak C-N stretching around 1020 cm^{-1}, maleimide and imide group at 686 cm^{-1} and 1386 cm^{-1} gets shifted to 794 cm^{-1}, 1016 cm^{-1}, 684 cm^{-1} and 1374 cm^{-1} respectively indicating better interaction MWCNT filler and BMI-epoxy matrix. Both the spectra retain the characteristic absorption bands of –C=O group at 1708 cm^{-1}, -C=C- of benzene ring at 1511 cm^{-1} and –C-N-C maleimide group at 1093 cm^{-1}. Very weak absorption bands indicating the presence of –C=C- stretching vibrations in MWCNT are observed in the range 2190-2230 cm^{-1} in BMI-epoxy-MWCNT composite with different fillers also emphasizes the better dispersion of MWCNT filler in the fabricated composites.

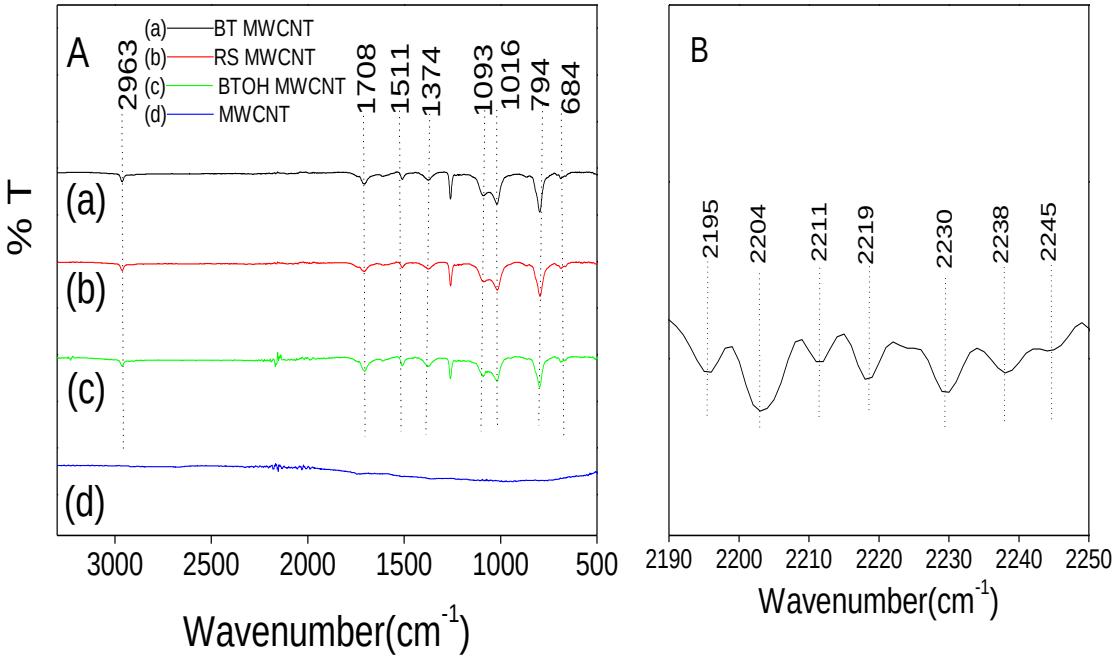

Figure 7.2 FTIR spectra of (A) BMI-epoxy-MWCNT composites with different fillers such as (a) BT, (b) RS, (c) BTOH and (d) pristine MWCNT (B) enlarged portion of –C=C- stretching vibrations in MWCNT.

7.2.3. Morphological studies

7.2.3.1. X-ray diffraction analysis

The X-ray diffractograms of BMI-epoxy-MWCNT composites with BT, RS and BTOH fillers and pristine MWCNT are displayed in figures 7.3(a), (b), (c) and (d) respectively. Typical XRD peaks of MWCNT obtained at 2θ around 26° and 43° corresponding to (002) and (100) planes were also visible in all other BMI-epoxy-MWCNT composites with different fillers indicating the effective dispersion of MWCNT in all the composites. The most intense peak around 31° corresponding to 110 plane of BTOH nanofiller is also visible in BMI-epoxy-MWCNT-BTOH nanocomposite with BTOH filler indicating more dispersion of this filler in the composite compared to other composites with BT and RS filler. The narrow diffraction peaks between the range 18°-21° of BMI-epoxy composite without filler are retained in XRD patterns of BMI-epoxy-MWCNT composites with different fillers[25–27].

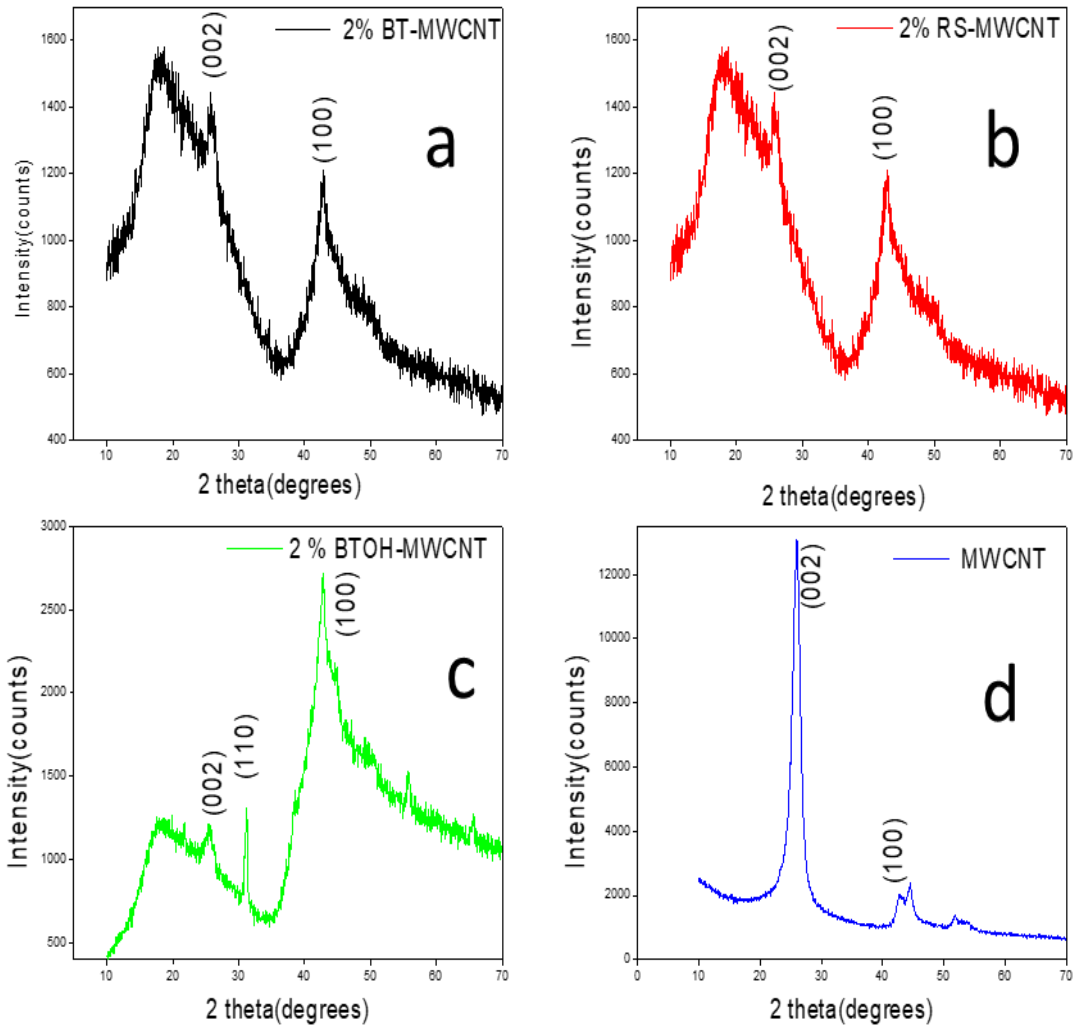

Figure 7.3 X-ray diffractograms of BMI-epoxy-MWCNT composites with 2 weight % of (a) BT, (b) RS, (c) BTOH fillers and (d) pristine MWCNT.

7.2.3.2. SEM –EDAX studies

Figure 7.4A depicts the SEM image of BMI-epoxy-MWCNT composite with 2 weight % of BT nanofiller. The presence of very small clusters may be due to the agglomeration owing to the strong van der Waal's interaction between the MWCNT nanofillers. EDAX spectra (figure 7.4B) and mapping (figure 7.5A) of BMI-epoxy-MWCNT composites with 2 weight % of BT nanofiller reveal the presence of all the elements present in the composite such as carbon (figure 7.5B), oxygen (figure 7.5C), titanium (figure 7.5D) and barium (figure 7.5E).

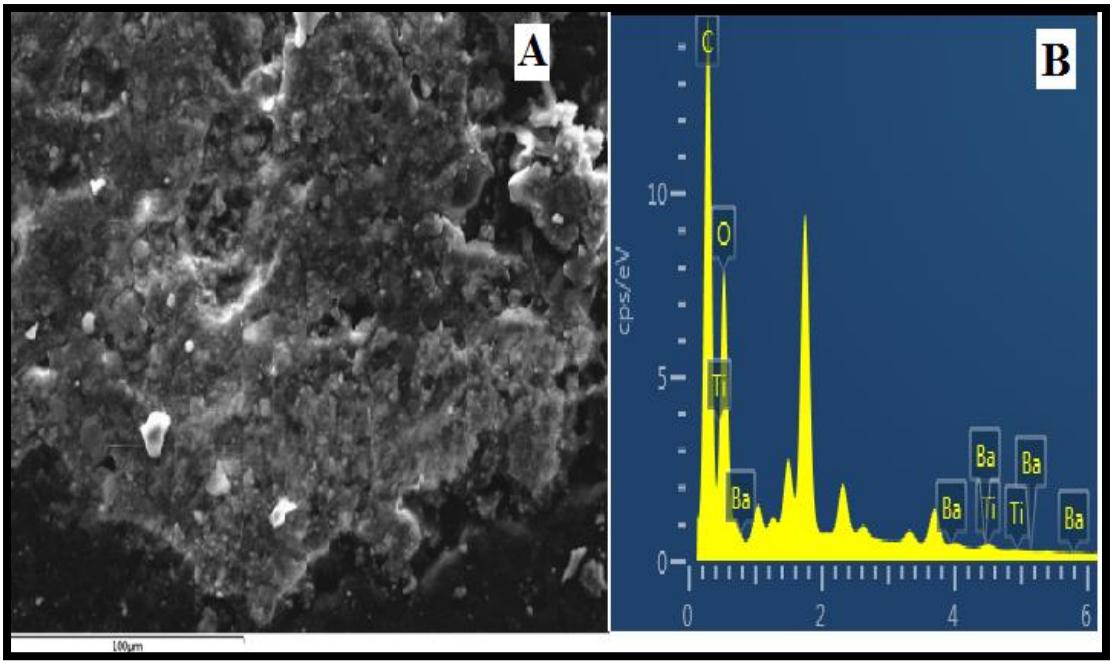

Figure 7.4 (A) SEM and (B) EDAX spectra of BMI-epoxy-MWCNT composites with 2 weight % of BT nanofiller.

Both loosely entangled MWCNT agglomerates along with river markings latter revealing the better dispersion of MWCNT can be seen in SEM images of BMI-epoxy-MWCNT composites with 2 weight % of RS filler (figure 7.6A)[28,29]. The presence of elements such as carbon (figure 7.7B), oxygen (figure 7.7C), potassium (figure 7.7D) and sodium (figure 7.7E) in the composite are further confirmed by EDAX spectra (figure 7.6B) and mapping (figure 7.7A) of BMI-epoxy-MWCNT composites with 2 weight % of RS filler.

Uniform dispersion of MWCNT nanofiller along with very small agglomerates are evident from SEM images of BMI-epoxy-MWCNT composites with 2 weight % of BTOH nanofiller (figure 7.8A)[30]. Presence of all the elements present in BMI-epoxy-MWCNT composites with 2 weight % of BTOH nanofiller such as carbon (figure 7.9B), oxygen (figure 7.9C), titanium (figure 7.9D) and barium (figure 7.9E) were identified and confirmed by EDAX spectra (figure 7.8B) and mapping (figure 7.9A).

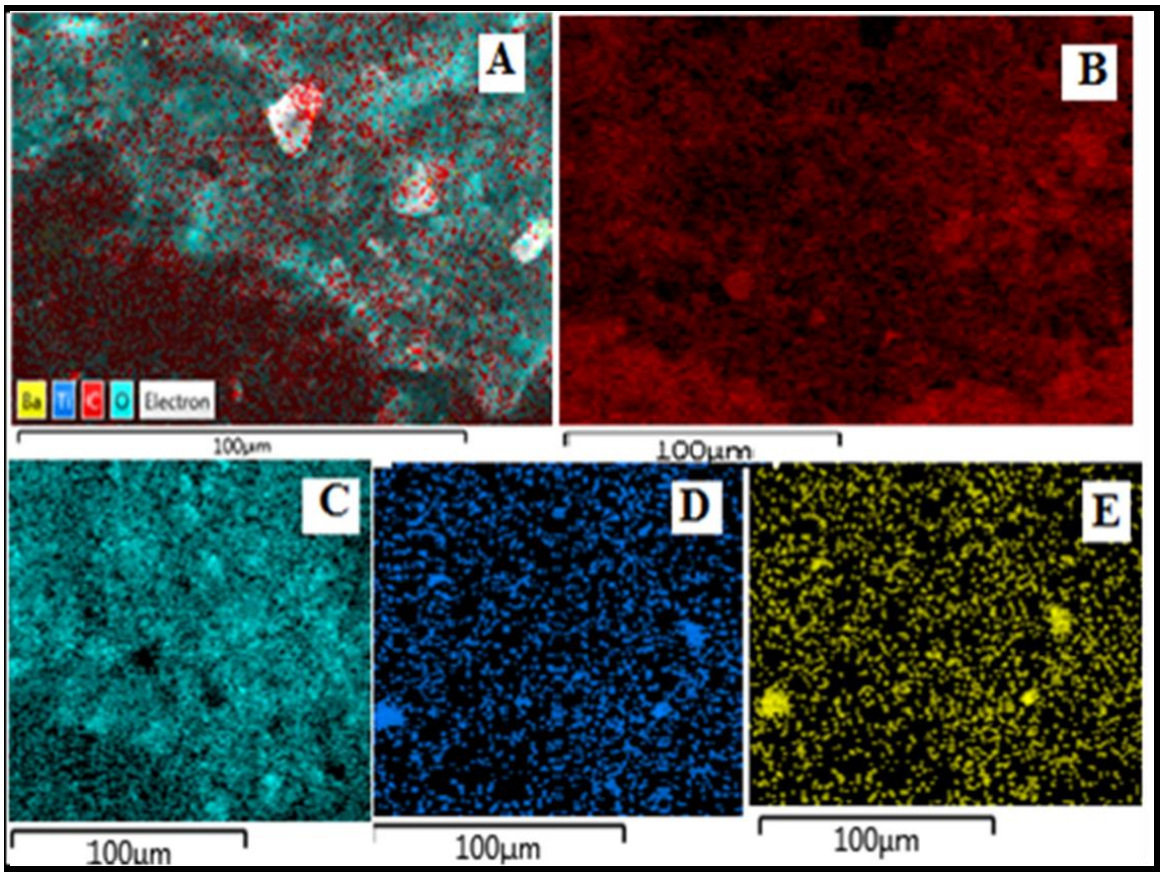

Figure 7.5 EDAX mapping of (A) BMI-epoxy-MWCNT composites with 2 weight % of BT nanofiller, (B) carbon, (C) oxygen, (D) titanium and (E) barium.

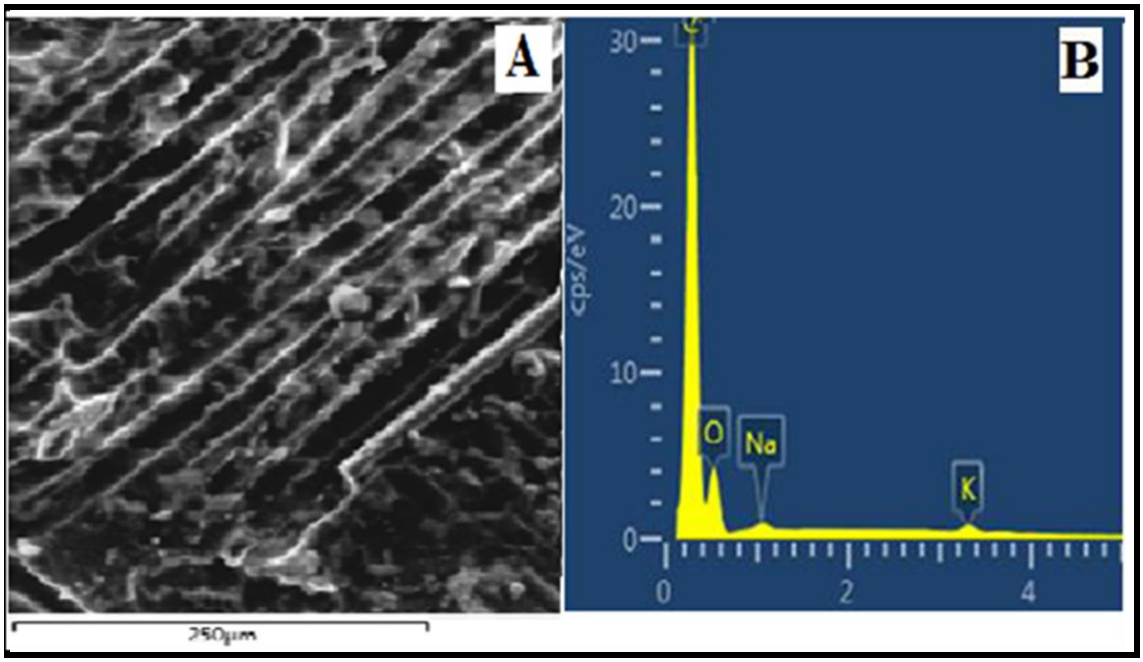

Figure 7.6 (A) SEM and (B) EDAX spectra of BMI-epoxy-MWCNT composites with 2 weight % of RS filler.

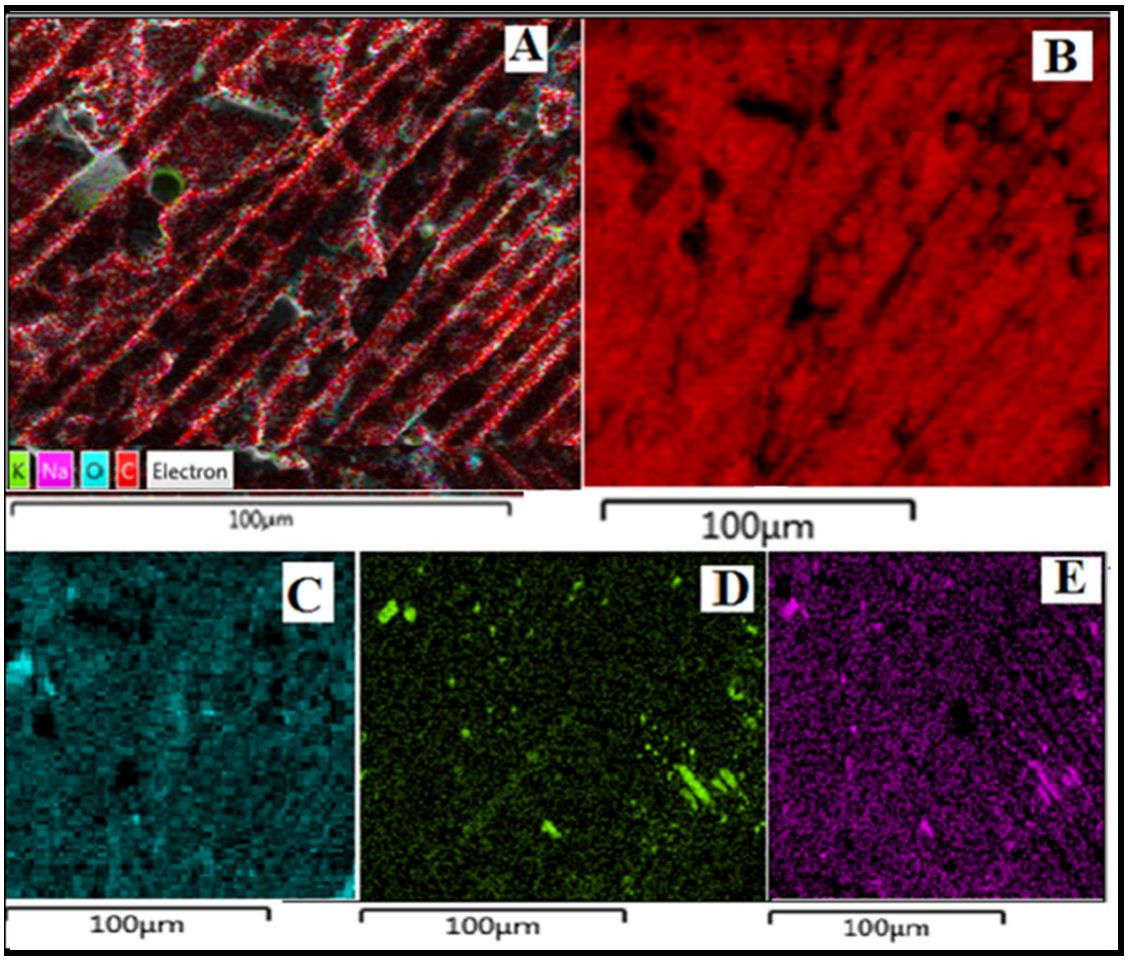

Figure 7.7 EDAX mapping of (A) BMI-epoxy-MWCNT composites with 2 weight % of RS nanofiller, (B) carbon, (C) oxygen, (D) potassium and (E) sodium.

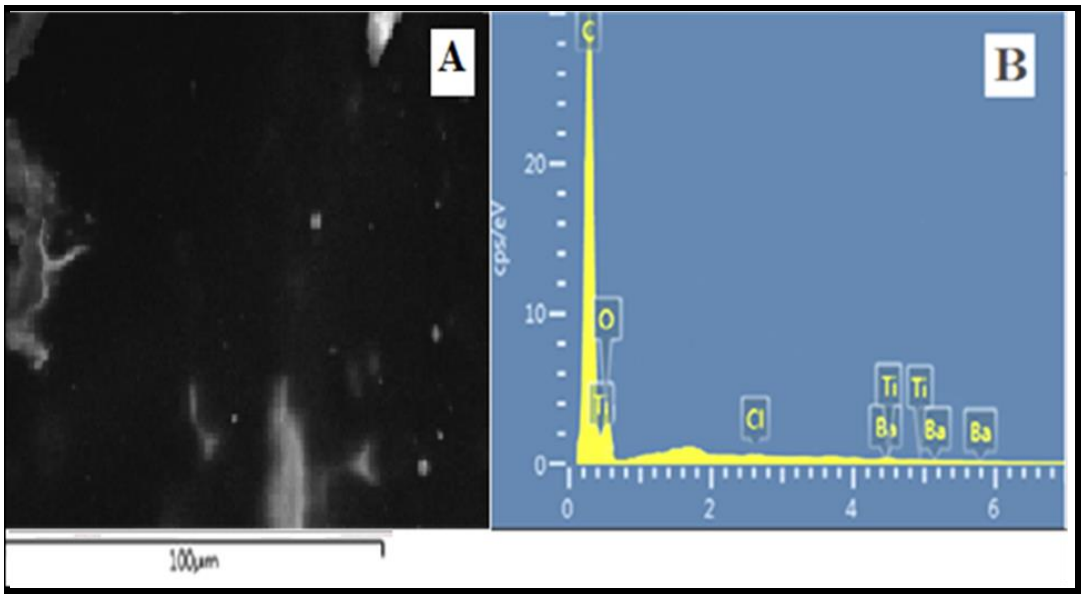

Figure 7.8 (A) SEM and (B) EDAX spectra of BMI-epoxy-MWCNT composites with 2 weight % of BTOH filler.

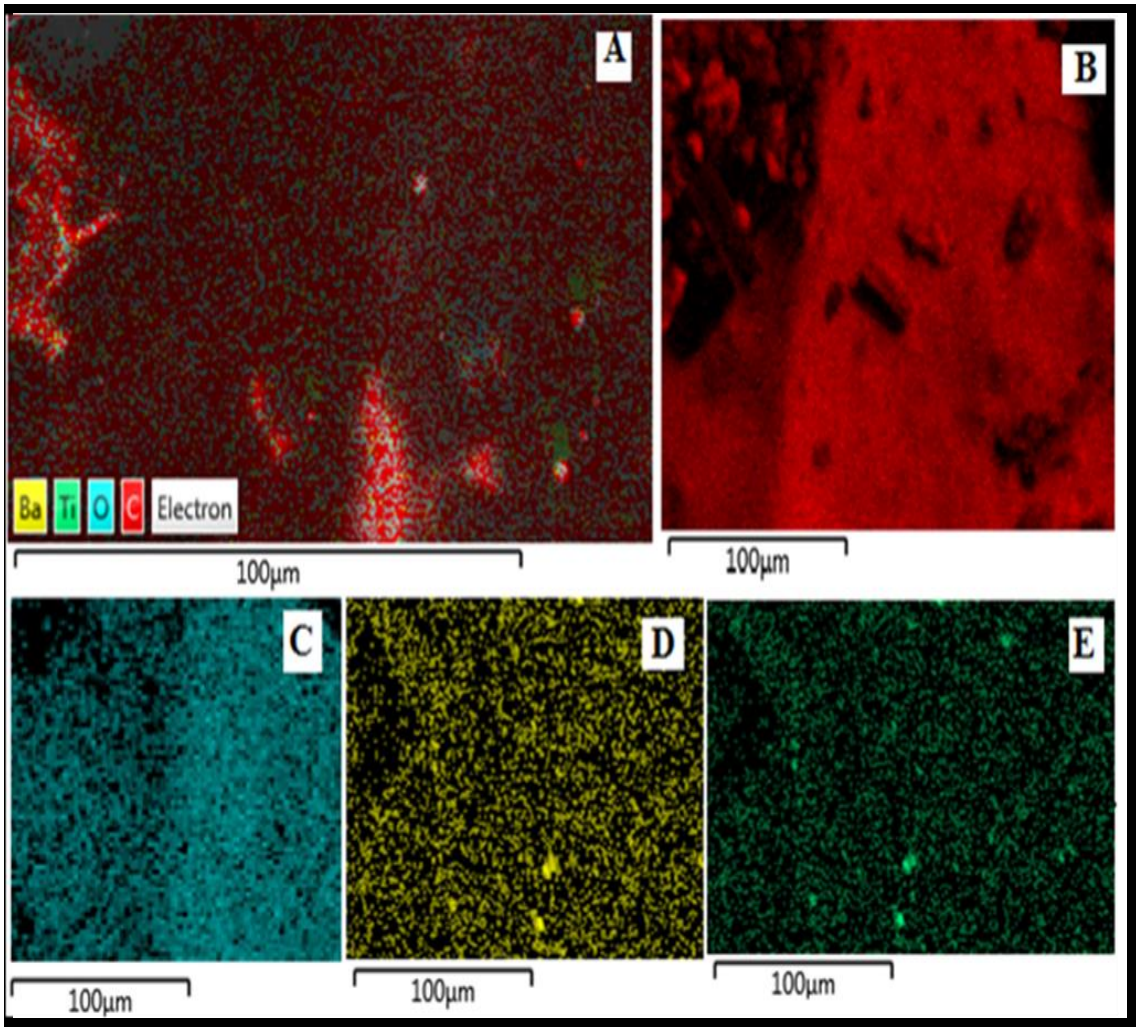

Figure 7.9 EDAX mapping of (A) BMI-epoxy-MWCNT composites with 2 weight % of BTOH nanofiller, (B) carbon, (C) oxygen, (D) barium and (E) titanium.

7.2.4. Mechanical properties

Figure 7.10 illustrates the effect of MWCNT nanofiller on tensile and flexural strength of BMI-epoxy composites with different fillers such as BT, RS and BTOH. The presence of a sharp peak at 2θ=30.96° corresponding to (110) plane in the XRD pattern of BMI-epoxy-MWCNT composite with BTOH nanofiller (figure 7.3 c) indicates the better dispersion of this nanofiller in BMI-epoxy-MWCNT matrix. This enhances the interaction between BMI-epoxy matrix and BTOH nanofiller resulting in improved mechanical properties of BMI-epoxy-MWCNT-BTOH nanocomposites compared to other composites[31,32].

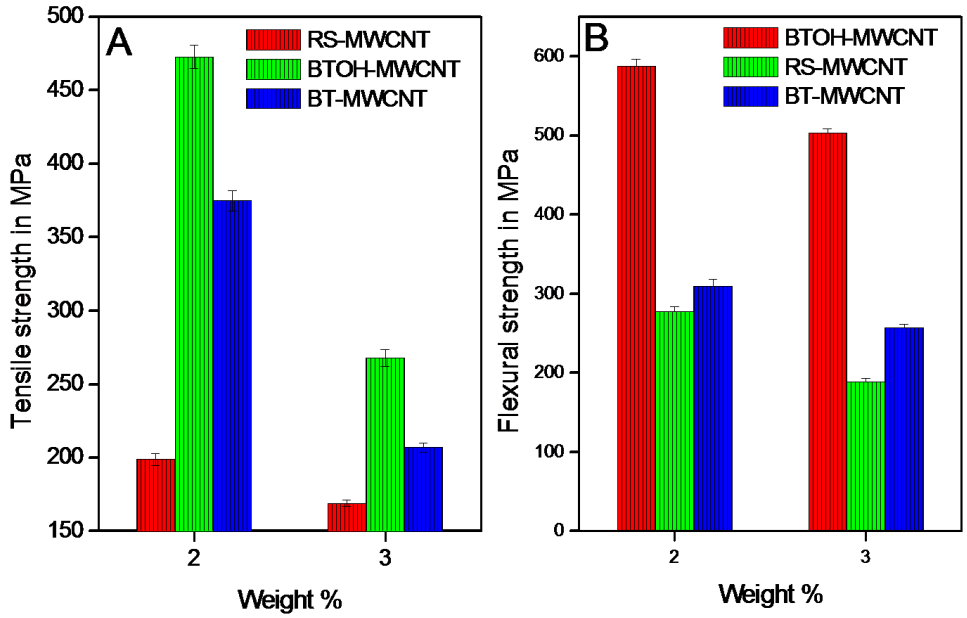

Figure 7.10 (A) Tensile and (B) flexural strength of BMI-epoxy-MWCNT composites with 2 weight % and 3 weight % of different nanofiller loadings.

7.2.5. Dielectric properties of BMI-epoxy-MWCNT composites

7.2.5.1. Dielectric permittivity

Variation of dielectric constant of all the BMI-epoxy composites with different fillers is depicted in figure 7.11. Among these, BMI-epoxy composites with 2 weight % of BTOH nanofiller exhibited highest dielectric constant and this may be due to the synergic effect arising from the increased interface interaction between BTOH nanofiller and BMI-epoxy matrix resulting in increased space charge polarization inside the nanocomposite[11]. This is further envisaged by the homogeneous SEM images (figure 10). Relatively high dielectric permittivity of BMI-epoxy-MWCNT composites with different fillers such as BT, RS and BTOH compared to BMI-epoxy composites without MWCNT filler is attributed to interfacial polarization between MWCNT and BMI-epoxy matrix[34–36]. Reduction in spacing between nanoparticles due to high loading of MWCNT conductive filler[37] and formation of a conductive network by MWCNT conductive filler in the composite result in the generation of a large number of mini-capacitors leading to greater enhancement in BMI-epoxy-MWCNT composite[38].

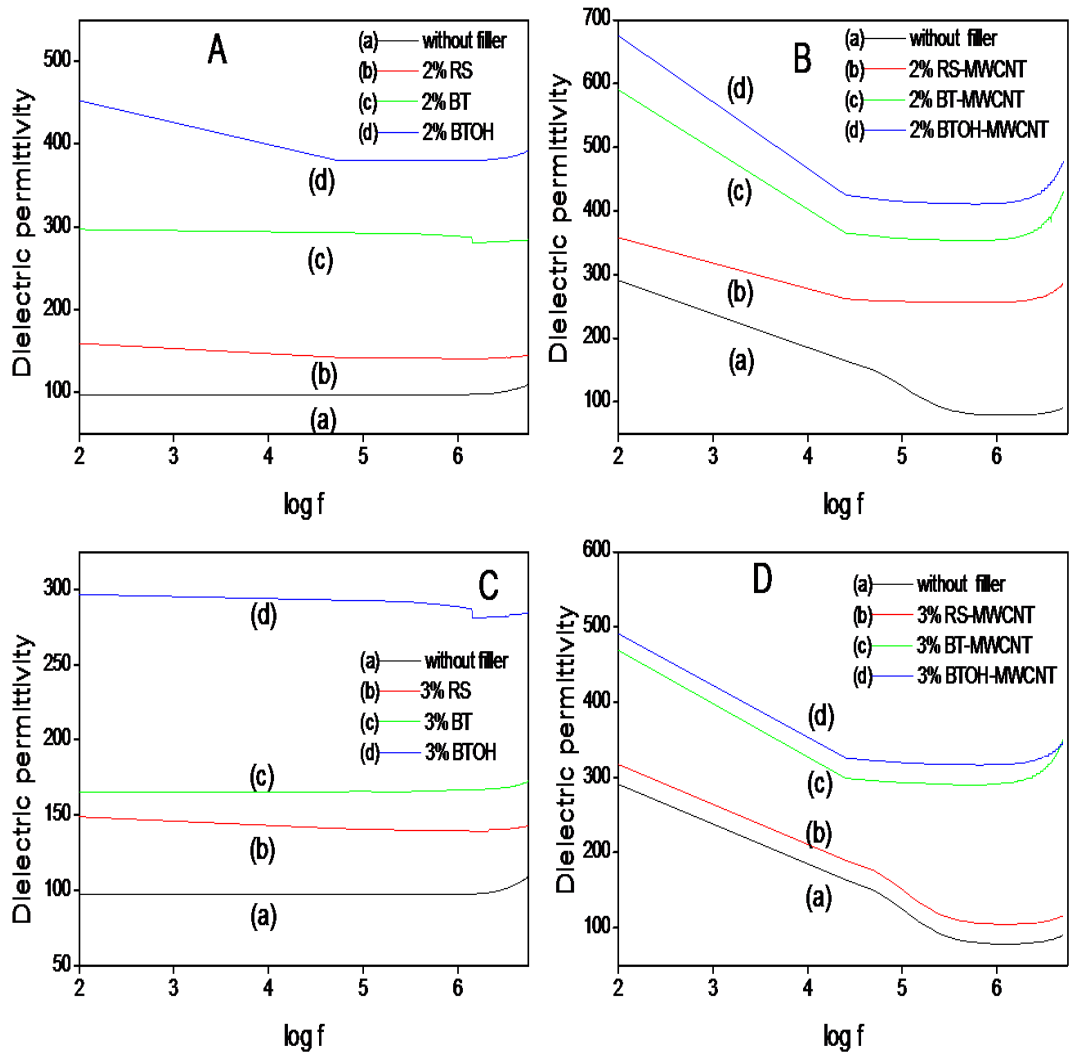

Figure 7.11 Variation of dielectric permittivity with the logarithmic frequency of SC-EGF reinforced BMI-epoxy nanocomposites with (A) (a) without filler, with 2 weight % of (b) RS, (c) BT and (d) BTOH (B) (a) without filler, with 2 weight % of (b) RS, (c) BT and (d) BTOH along with 5 % of MWCNT filler (C) (a) without filler, with 3 weight % of (b) RS, (c) BT and (d) BTOH (D) (a) without filler, with 3 weight % of (b) RS, (c) BT and (d) BTOH along with 5 % of MWCNT filler.

7.2.5.2. Dielectric loss (tan delta)

Figure 7.12 A and C represents the variation of dielectric loss with an applied frequency of the three types of BMI-epoxy composites with 2 and 3 weight % of different nanofillers and without filler. In order to exhibit better insulating properties, the dielectric loss of the composite should be as low as possible. In all the BMI-epoxy composites with BT, RS and BTOH fillers, dielectric loss decreases with an increase in

frequency. BMI-epoxy composite with BTOH nanofiller shows the lowest dielectric loss compared to RS and BT composites[39]. Among the BTOH filler added BMI-epoxy composites, the dielectric loss value is least for 2 weight % of BTOH that is highly attractive for sophisticated applications.

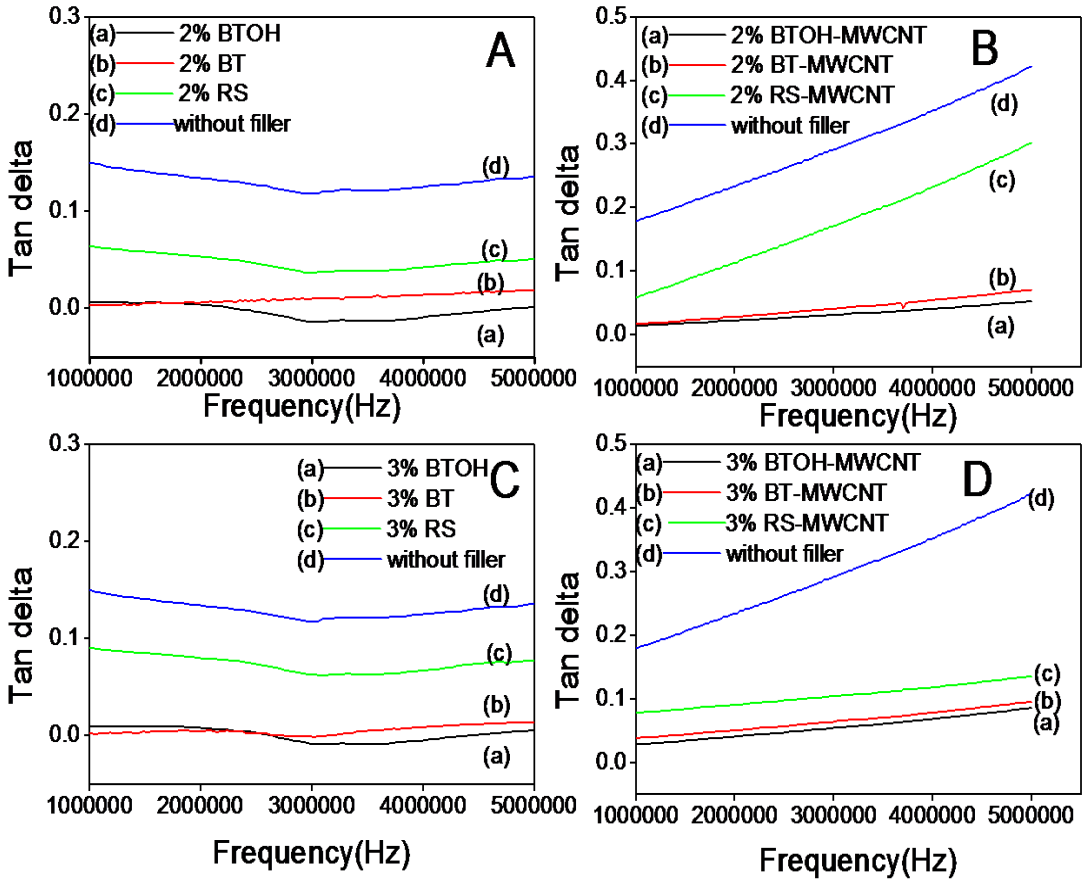

Figure 7.12 Variation of dielectric loss (tan delta) with frequency of SC-EGF reinforced BMI-epoxy nanocomposites with (A) (d) without filler, with 2 weight % of (a) BTOH, (b) BT, (c) RS and (B) (d) without filler, with 2 weight % of (a) BTOH, (b) BT and (c) RS along with 5 weight % of MWCNT filler (C) (d) without filler, with 3 weight % of (a) BTOH, (b) BT and (c) RS (D) (d) without filler, with 3 weight % of (a) BTOH, (b) BT and (c) RS along with 5 weight % of MWCNT filler.

From figure 7.12 B and D, it is observed that BMI-epoxy composites with MWCNT filler exhibited a slight increase in dielectric loss value as compared to those without MWCNT filler is due to the formation of conductive paths and change in the nature of composites from dielectric to conducting which result in leakage current leading to high dielectric loss[40–42].

7.2.5.3. Dielectric strength

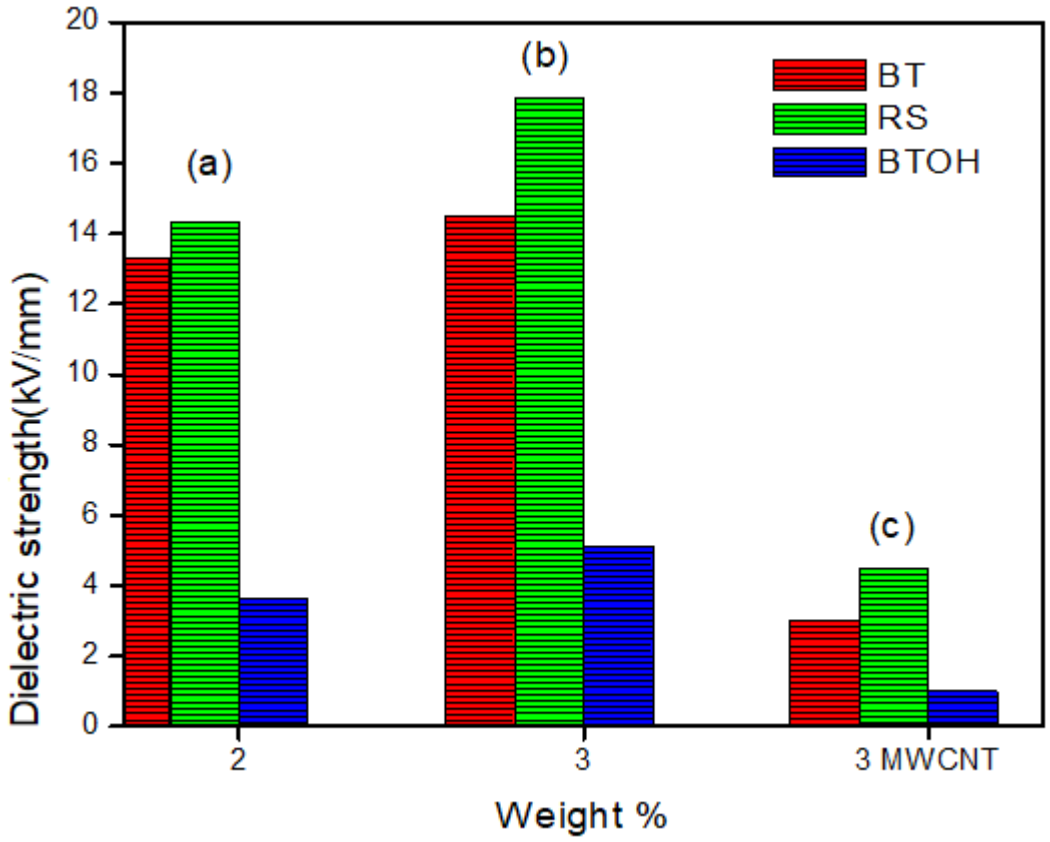

Figure 7.13 Variation of dielectric strength with filler % of SC-EGF reinforced BMI-epoxy nanocomposites with (a) 2 weight % of BT, RS, BTOH,(b) 3 weight % of BT, RS, BTOH and (c) 3 weight % of BT, RS, BTOH with MWCNT filler.

The variation of dielectric strength on 2 and 3 weight % of different nanofillers incorporated in BMI-epoxy composites are illustrated in figure 7.13. The increase in dielectric strength with 3 weight % of nanofiller is attributed to the decrease in mobility of the polymer chains thereby reducing the probability of transferring charge carriers through the polymer chains that are not directly bonded to the nanofillers[13]. Among the BMI-epoxy composites with 2 and 3 weight % of different nanofillers, the one with 3 weight % of RS filler exhibited the highest values of dielectric strength that may be due to the suppression of space charge transfer[14]. Due to the increased interface compatibility between the BMI-epoxy matrix and BTOH nanoparticle, the probability of charge transfer is more in this composite compared to BMI-epoxy composite with BT filler leading to decrease in dielectric strength in BMI-epoxy BTOH composite.

From figure 7.13 c it is observed that BMI-epoxy-MWCNT composite 3 weight % of RS filler exhibited the highest values of dielectric strength.

7.2.6. AC conductivity studies

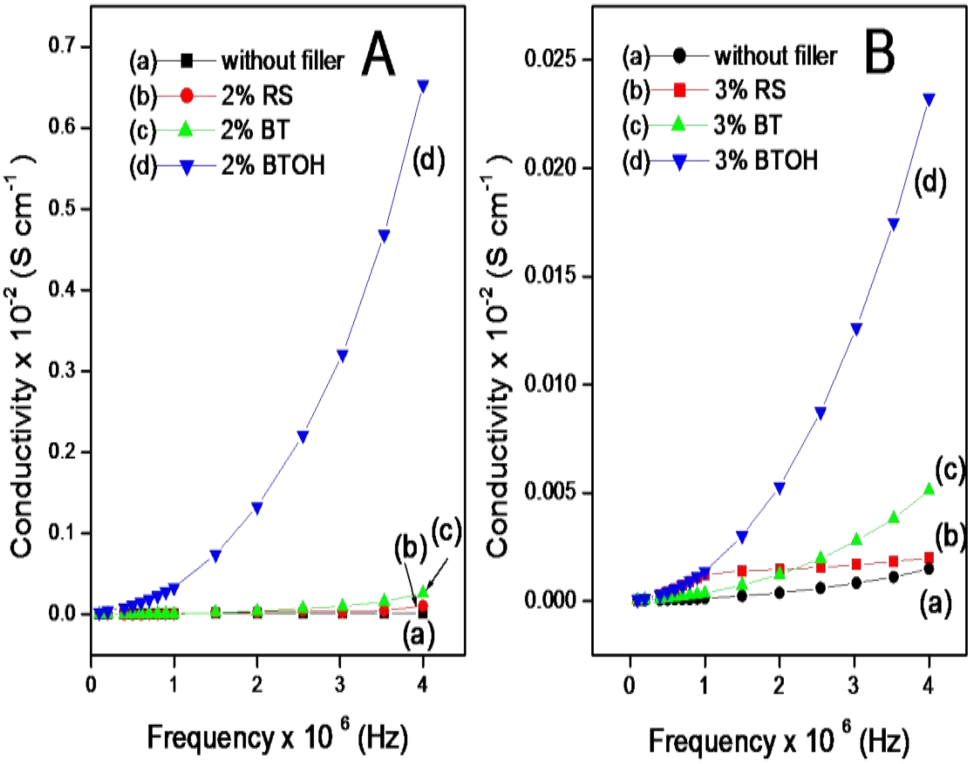

Figure 7.14 Comparison of ac conductivities of BMI-epoxy composites with (A) (a) without filler, with 2 weight % of (b) RS, (c) BT and (d) BTOH filler (B) (a) without filler, with 3 weight % of (b) RS, (c) BT and (d) BTOH filler.

The magnitude of AC conductivity values of BMI-epoxy composites with different nanofillers are calculated using the formula: $\sigma = \omega \epsilon_r \epsilon_0 \tan \delta$, where ω is the angular frequency, ϵ_r is the dielectric constant of the composite, ϵ_0 is dielectric permittivity in free space and $\tan \delta$ is the dielectric loss. From figure 7.14, it is evident that the ac conductivity of BMI-epoxy composites with 2 and 3 weight % of BT and RS fillers show very low conductivity compared to composites with the same weight % of BTOH nanofiller, the latter shows a gradual increase in conductivity.

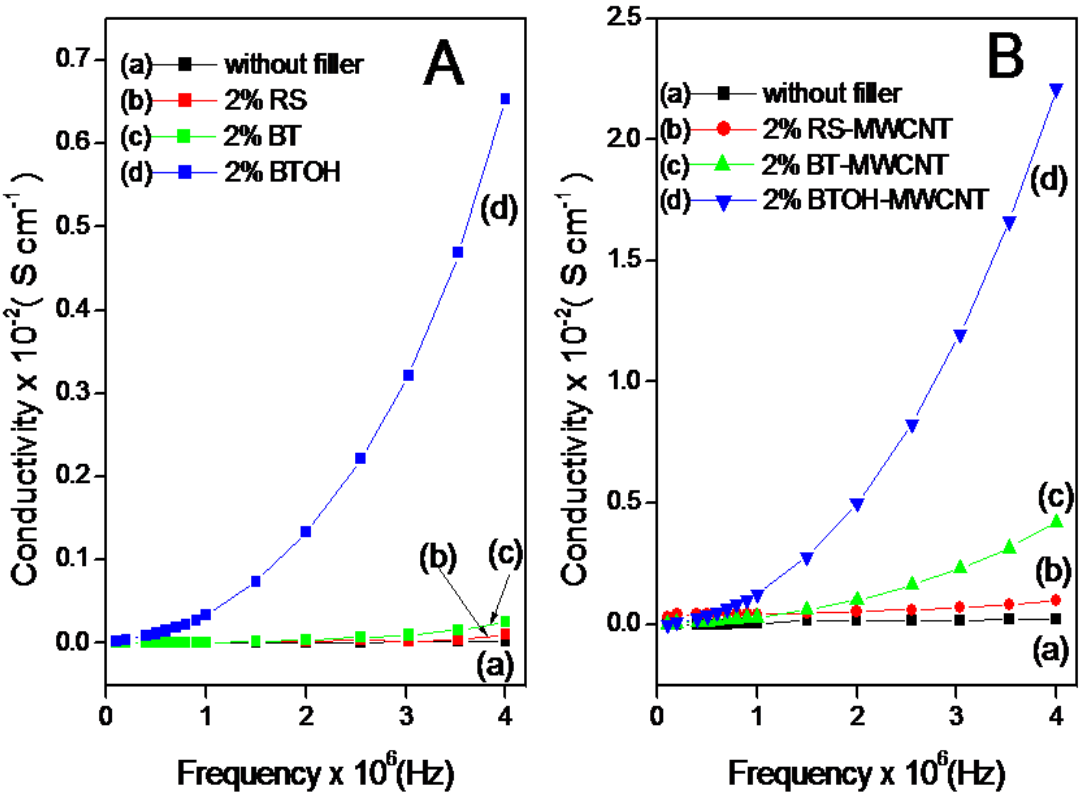

Figure 7.15 Comparison of ac conductivity of BMI-epoxy composites with 2 weight % of (A) (a) without any fillers, with (b) RS, (c) BT and (d) BTOH filler and (B) BMI-epoxy-MWCNT composite (a) without any fillers, with (b) RS (c) BT and (d) BTOH filler.

The increase in ac conductivity of BMI-epoxy-BTOH composites may be attributed to the greater interaction between -OH group of BTOH nanoparticle with BMI-epoxy composite that may lead to a reduction in charge trapping thereby producing a conductive path through the BMI-epoxy matrix resulting in increased ac conductivity compared to other composites. Among the three fillers, BT, RS and BTOH, RS particles are more insulated than other fillers, further supported by high dielectric breakdown values observed in BMI-epoxy composites with RS filler (figure 7.13). The presence of insulated RS particles will prevent the migration of electrons in the composites thereby preventing the formation of a conductive path in the composites[45]. BMI-epoxy-MWCNTcomposites with different fillers exhibited higher conductivity compared to BMI-epoxy composites without MWCNT filler due to the presence of conductive MWCNT filler in the composites.

7.2.7. EMI shielding effectiveness(EMI-SE)

The variation of EMI shielding effectiveness of the fabricated BMI-epoxy composites with 2 and 3 weight % of BT, RS and BTOH fillers in the X band range are illustrated in figure 7.16. The maximum value of EMI shielding effectiveness is exhibited by BMI-epoxy composites with 2 and 3 weight % of BTOH filler are 2.5 and 1.85 respectively at 8 GHz.

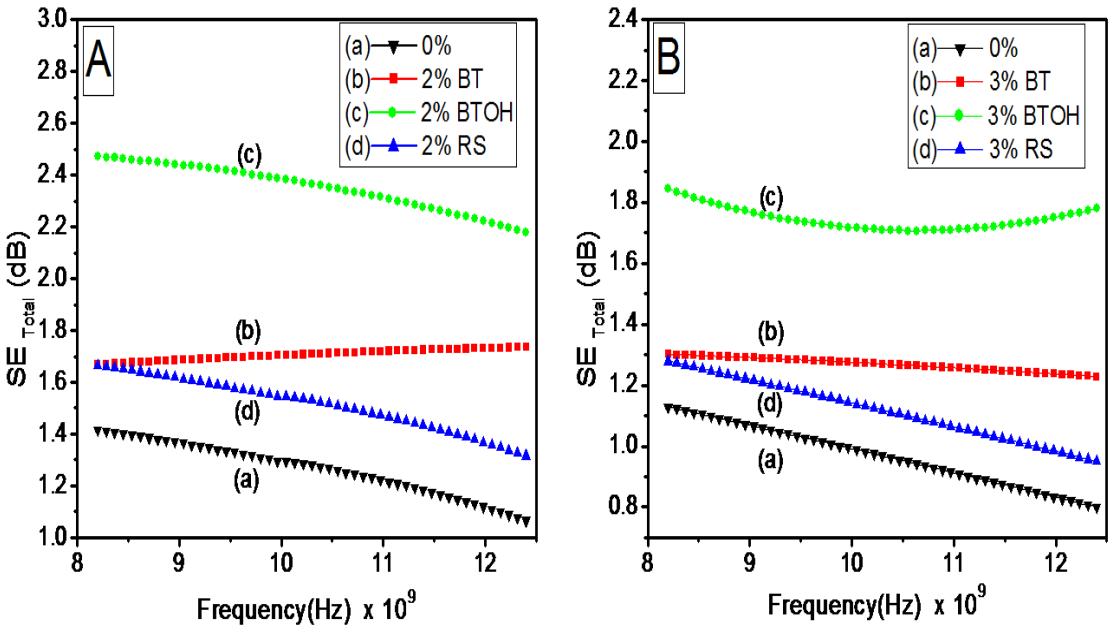

Figure 7.16 Comparison of EMI shielding effectiveness of BMI-epoxy composites with (A) 2 weight % and (B) 3 weight % of (b) BT, (c) BTOH, (d) RS fillers and (a) without any fillers.

Polymer nanocomposites with at least 20 dB of EMI shielding effectiveness are required for shielding applications. So these fabricated BMI-epoxy composites that are not suitable for shielding applications can be made so by incorporating suitable conducting nanofillers like CNTs into the matrix[15,46].

The variation of EMI shielding effectiveness of the fabricated BMI-epoxy composites with 2 weight % of BT, RS and BTOH fillers in the K band range are illustrated in figure 7.17A. The maximum value of EMI shielding effectiveness exhibited by BMI-epoxy composites with 2 weight % of BTOH filler in BMI-epoxy composites without and with MWCNT (figure 7.17 B) are 8.2 and 14.3 respectively at 26 GHz.

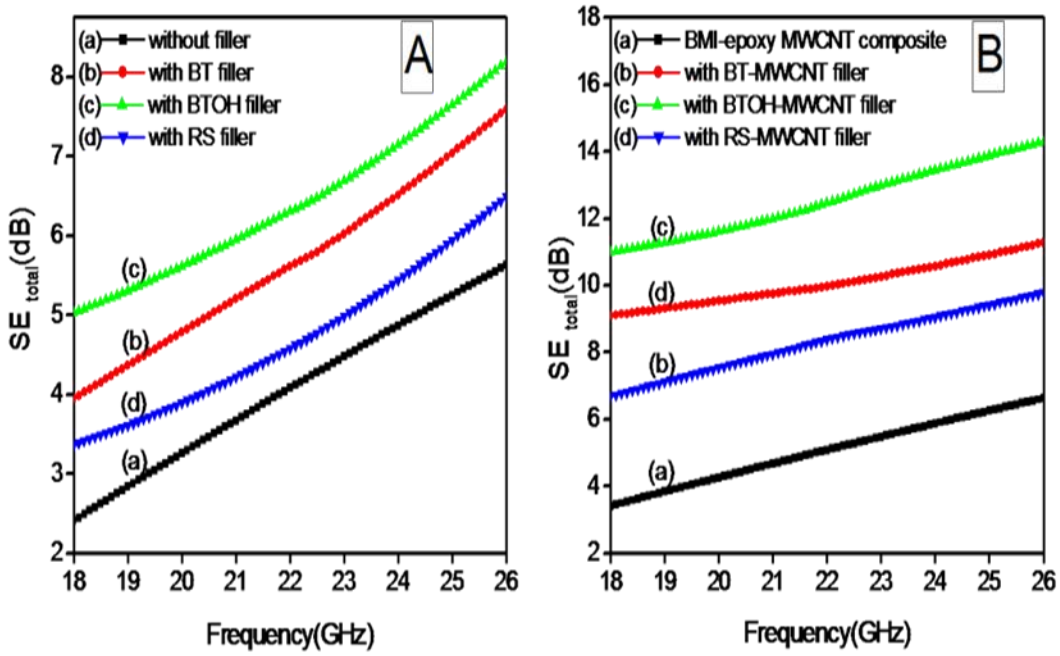

Figure 7.17 Comparison of EMI shielding effectiveness of BMI-epoxy composites with 2 weight % of (A) (b) BT, (c) BTOH, (d) RS fillers and (a) without any fillers and (B) BMI-epoxy-MWCNT composite (a) without any fillers, with (b) BT, (c) BTOH, (d) RS filler.

7.3. Conclusions

In this research work, we explored the possibility to enhance the thermo-mechanical, dielectric and EMI-SE of BMI-epoxy composites for high dielectric applications by incorporating different fillers such as BT, RS and BTOH with conductive filler, MWCNT. In this study, we maintain the concentration of BMI-epoxy constant and varied the concentration of different fillers such as BT, RS and BTOH during the fabrication of BMI-epoxy composites and quantified the concentration of filler required for high dielectric permittivity and low dielectric loss. The optimized weight % of the fillers determined were 2 and 3 weight %. These compositions were selected for the fabrication of another series of BMI-epoxy composites with a constant concentration of MWCNT (5 weight %) using a simple hand layup method followed by compression moulding and characterized to explore the influence of MWCNT filler on thermo-mechanical, dielectric and EMI-SE of the fabricated composites.

Tensile strength, flexural strength and dielectric permittivity of BMI-epoxy-MWCNT nanocomposite with 2 weight % of BTOH nanofiller were increased 2.78, 1.22 and 1.50

times respectively as compared to BMI-epoxy-BTOH nanocomposite without MWCNT filler. The highest dielectric permittivity of around 674 and minimum value of dielectric loss of 0.017 was obtained for BMI-epoxy-MWCNT composite with 2 weight % of BTOH nanofiller and this composite stands as a promising candidate for high dielectric applications.

Based on the above results, it can be envisaged that MWCNT filler can act as an excellent modifier to enhance thermo-mechanical, dielectric properties, ac conductivity as well as EMI-SE of the fabricated BMI-epoxy composites with different fillers for use in high dielectric application devices such as capacitors, insulating and dielectric materials.

References

1. Basuli, U., Chattopadhyay, S., Nah, C. & Chaki, T. K. Electrical properties and electromagnetic interference shielding effectiveness of multiwalled carbon nanotubes-reinforced EMA nanocomposites. Polym. Compos. 33, 897–903 (2012).
2. Gupta, A. & Choudhary, V. Electrical conductivity and shielding effectiveness of poly (trimethylene terephthalate)/multiwalled carbon nanotube composites. J. Mater. Sci. 46, 6416–6423 (2011).
3. Jou, W.-S., Cheng, H.-Z. & Hsu, C.-F. The electromagnetic shielding effectiveness of carbon nanotubes polymer composites. J. Alloys Compd. 434, 641–645 (2007).
4. Park, S. H., Thielemann, P., Asbeck, P. & Bandaru, P. R. Enhanced dielectric constants and shielding effectiveness of uniformly dispersed functionalized carbon nanotube composites. Appl. Phys. Lett. 94, 239–241 (2009).
5. Arjmand, M., Apperley, T., Okoniewski, M. & Sundararaj, U. Comparative study of electromagnetic interference shielding properties of injection molded versus compression molded multi-walled carbon nanotube/polystyrene composites. Carbon N. Y. 50, 5126–5134 (2012).
6. Huang, Y. et al. The influence of single-walled carbon nanotube structure on the electromagnetic interference shielding efficiency of its epoxy composites. Carbon N. Y. 45, 1614–1621 (2007).
7. Gelves, G. A., Al-Saleh, M. H. & Sundararaj, U. Highly electrically conductive and high performance EMI shielding nanowire/polymer nanocomposites by miscible mixing and precipitation. J. Mater. Chem. 21, 829–836 (2011).
8. Al-Saleh, M. H., Gelves, G. A. & Sundararaj, U. Copper nanowire/polystyrene nanocomposites: lower percolation threshold and higher EMI shielding. Compos. Part A Appl. Sci. Manuf. 42, 92–97 (2011).
9. Al-Saleh, M. H. & Sundararaj, U. A review of vapor grown carbon nanofiber/polymer conductive composites. Carbon N. Y. 47, 2–22 (2009).
10. Al-Saleh, M. H. & Sundararaj, U. Electrically conductive carbon nanofiber/polyethylene composite: effect of melt mixing conditions. Polym. Adv. Technol. 22, 246–253 (2011).
11. Al-Saleh, M. H. & Sundararaj, U. Morphological, electrical and electromagnetic interference shielding characterization of vapor grown carbon nanofiber/polystyrene nanocomposites. Polym. Int. 62, 601–607 (2013).
12. Al-Saleh, M. H. & Sundararaj, U. X-band EMI shielding mechanisms and shielding effectiveness of high structure carbon black/polypropylene composites. J. Phys. D. Appl. Phys. 46, 35304 (2012).
13. Hsieh, C.-T., Pan, Y.-J. & Lin, J.-H. Polypropylene/high-density polyethylene/carbon

fiber composites: manufacturing techniques, mechanical properties, and electromagnetic interference shielding effectiveness. Fibers Polym. 18, 155–161 (2017).
14. Luo, X. & Chung, D. D. L. Electromagnetic interference shielding using continuous carbon-fiber carbon-matrix and polymer-matrix composites. Compos. Part B Eng. 30, 227–231 (1999).
15. Al-Saleh, M. H., Saadeh, W. H. & Sundararaj, U. EMI shielding effectiveness of carbon based nanostructured polymeric materials: A comparative study. Carbon N. Y. 60, 146–156 (2013).
16. Chung, D. D. L. Carbon materials for structural self-sensing, electromagnetic shielding and thermal interfacing. Carbon N. Y. 50, 3342–3353 (2012).
17. Dhawan, S. K., Ohlan, A. & Singh, K. Designing of nanocomposites of conducting polymers for EMI shielding. (InTech, 2011).
18. Muzaffar, A., Ahamed, M. B., Deshmukh, K. & Faisal, M. Electromagnetic interference shielding properties of polyvinylchloride (PVC), barium titanate ($BaTiO_3$) and nickel oxide (NiO) based nanocomposites. Polym. Test. 77, (2019).
19. Cheng, Q., Wang, B., Zhang, C. & Liang, Z. Functionalized carbon-nanotube sheet/bismaleimide nanocomposites: Mechanical and electrical performance beyond carbon-fiber composites. Small 6, 763–767 (2010).
20. Iijima, S. Helical microtubules of graphitic carbon. Nature 354, 56–58 (1991).
21. Iijima, S. & Ichihashi, T. Single-shell carbon nanotubes of 1-nm diameter. Nature 363, 603–605 (1993).
22. Gu, A., Liang, G., Liang, D. & Ni, M. Bismaleimide/carbon nanotube hybrids for potential aerospace application: I. Static and dynamic mechanical properties. Polym. Adv. Technol. 18, 835–840 (2007).
23. Park, D., Ju, H., Oh, T. & Kim, J. A p-type multi-wall carbon nanotube/Te nanorod composite with enhanced thermoelectric performance. RSC Adv. 8, 8739–8746 (2018).
24. Vellingiri, L., Annamalai, K., Kandasamy, R. & Kombiah, I. Synthesis and characterization of MWCNT impregnated with different loadings of SnO2 nanoparticles for hydrogen storage applications. Int. J. Hydrogen Energy 43, 848–860 (2018).
25. Nie, P. et al. Preparation and tribological properties of polyimide/carboxyl-functionalized multi-walled carbon nanotube nanocomposite films under seawater lubrication. Tribol. Lett. 58, 1–12 (2015).
26. Lee, D. Y. et al. Effect of multiwalled carbon nanotube (M-CNT) loading on M-CNT distribution behavior and the related electromechanical properties of the M-CNT dispersed ionomeric nanocomposites. Surf. Coatings Technol. 200, 1920–1925 (2005).
27. Fathi, Z., Khavari Nejad, R. A., Mahmoodzadeh, H. & Satari, T. N. Investigating of a wide range of concentrations of multi-walled carbon nanotubes on germination and growth of castor seeds (Ricinus communis L.). J. Plant Prot. Res. 57, 228–236 (2017).
28. Ma, P. C., Kim, J.-K. & Tang, B. Z. Effects of silane functionalization on the properties of carbon nanotube/epoxy nanocomposites. Compos. Sci. Technol. 67, 2965–2972 (2007).
29. Costa, P. On the use of surfactants for improving nanofiller dispersion and piezoresistive response in stretchable polymer composites. J. Mater. Chem. C 6, 10580--10588 (2018).
30. Ma, P. C. et al. Enhanced electrical conductivity of nanocomposites containing hybrid fillers of carbon nanotubes and carbon black. ACS Appl. Mater. Interfaces 1, 1090–1096 (2009).
31. Jayakrishnan, M. T. R. P. Role of Nickel Oxide Nanoparticles on Magnetic, Thermal and Temperature Dependent Electrical Conductivity of Novel Poly (vinyl cinnamate) Based Nanocomposites : Applicability of Different Conductivity Models. J. Inorg. Organomet. Polym. Mater. (2016) doi:10.1007/s10904-016-0456-x.
32. Karakoti, A., Soundhar, A., Rajesh, M., Jayakrishna, K. & Sultan, M. T. B. H. H. Enhancement of mechanical properties of an epoxy composite reinforced with Hibiscuss sabdariffa var. Altissima fiber micro cellulose. Int. J. Recent Technol. Eng. 8, 477–480 (2019).
33. Moharana, S., Mishra, M. K., Behera, B. & Mahaling, R. N. Enhanced Dielectric Properties of Polyethylene Glycol (PEG) Modified $BaTiO_3$ (BT) -Poly (vinylidene

fluoride) (PVDF). Polym. Sci. A 59, 405–415 (2017).
34. Luo, H. et al. Methoxypolyethylene glycol functionalized carbon nanotube composites with high permittivity and low dielectric loss. Compos. Part A Appl. Sci. Manuf. 86, 57–65 (2016).
35. Dang, Z.-M., Yao, S.-H., Yuan, J.-K. & Bai, J. Tailored dielectric properties based on microstructure change in $BaTiO_3$-carbon nanotube/polyvinylidene fluoride three-phase nanocomposites. J. Phys. Chem. C 114, 13204–13209 (2010).
36. Hayashida, K. Special Feature : Organic Materials Electrical Properties of Polymethacrylate-grafted Carbon Nanotube Composites Prepared Using Surface-initiated Polymerization. 44, 35–43 (2013).
37. Wang, R. et al. Preparation and properties of MWCNTs-BNNSs/epoxy composites with high thermal conductivity and low dielectric loss. Mater. Today Commun. 24, (2020).
38. Song, Y., Noh, T. W., Lee, S.-I. & Gaines, J. R. Experimental study of the three-dimensional ac conductivity and dielectric constant of a conductor-insulator composite near the percolation threshold. Phys. Rev. B 33, 904 (1986).
39. Kuo, D.-H., Chang, C.-C., Su, T.-Y., Wang, W.-K. & Lin, B.-Y. Dielectric behaviours of multi-doped $BaTiO_3$/epoxy composites. J. Eur. Ceram. Soc. 21, 1171–1177 (2001).
40. Song, S. et al. A facile strategy to enhance the dielectric and mechanical properties of MWCNTs/PVDF composites with the aid of MMA-co-GMA copolymer. Materials (Basel). 11, (2018).
41. Ameli, A., Nofar, M., Park, C. B., Pötschke, P. & Rizvi, G. Polypropylene/carbon nanotube nano/microcellular structures with high dielectric permittivity, low dielectric loss, and low percolation threshold. Carbon N. Y. 71, 206–217 (2014).
42. Wang, J. et al. Enhancing dielectric performance of poly(vinylidene fluoride) nanocomposites via controlled distribution of carbon nanotubes and barium titanate nanoparticles. Eng. Sci. 4, 76–86 (2018).
43. Song, Y. et al. Enhanced dielectric and ferroelectric properties induced by dopamine-modified $BaTiO_3$ nanofibers in flexible poly (vinylidene fluoride-trifluoroethylene) nanocomposites. J. Mater. Chem. 22, 8063–8068 (2012).
44. Ma, D. et al. Influence of nanoparticle surface modification on the electrical behaviour of polyethylene nanocomposites. Nanotechnology 16, 724–731 (2005).
45. Yang, J. hui et al. Graphene oxide-tailored dispersion of hybrid barium titanate@polypyrrole particles and the dielectric composites. Chem. Eng. J. 355, 137–149 (2019).
46. Wei, H. G. et al. Multifunctions of Polymer Nanocomposites: Environmental Remediation, Electromagnetic Interference Shielding, And Sensing Applications. ChemNanoMat 6, 174–184 (2020).